Numerical study of turbulent flow over complex topography by LES model

Zhenqing Liu*[1)], Takeshi Ishihara**[2)]

1,2)Department of Civil Engineering, The University of Tokyo, Tokyo, Japan,
**) Zhenqing Liu, liu@bridge.t.u-tokyo.ac.jp*
***) Takeshi Ishihara, ishihara@bridge.t.u-tokyo.ac.jp*

ABSTRACT

The present work is devoted to develop a numerical wind tunnel to study the local turbulent flow fields over complex topography by using large eddy simulation. Firstly, the mean and turbulence flow over flat terrain and that over a steep 3-dimensional circular hill were simulated and the accuracy of these computations was assessed by comparing the results with those from the experiment. Then the simulations about a real complex topography with two different radius were carried out and the comparison with observation shows that, even the measured point is located with a distance 10 times the height of an upstream tall hill, the wake effect is still very large and in order to provide a good prediction that tall hill should be included in the simulated region.

1 INTRODUCTION

Modelling of turbulent wind field over complex topography is of great interest in many engineering applications. For example, the site selection for extracting wind energy, assessment of the safety of structure built on complex terrain, air pollution prediction in mountain area, etc. Several numerical studies by using k-ε model (e.g., Kobayashi et al., 1994; Ferreira et al., 1995; Ishihara and Hibi, 2002) have been conducted, and it has been found that the revised form of k-ε model, such as Shin's model, gives rise to more comparable results with experiment than Standard k-ε model for both mean flow and turbulence. However, by using k-ε model the instantaneous characteristics of the flow could not be captured. Therefore, in the last decade LES turbulence model was tried in some researches (e.g., Tamura et al., 2007; Dupont et al., 2008; Cao et al., 2012), providing some valuable information about the mechanism of the flow over a simple 3-D hill or 2-D ridge. For the flow over a real complex hill, LES model has also been tried in the works by Lopes et al. (2007) and Diebold et al. (2013), however, the surrounding region of the hill studied is not so mountainous and the hill is not so steep compared with most hills in Japan.

This study aims to develop a numerical wind tunnel to study the local turbulent flow fields over complex topography by using large eddy simulation. Three cases, flat terrain, 3-D hill, and real complex terrain in Japan, will be studied. Section 2 will introduce the governing equations. The details of the numerical model for the three cases will be introduced in Section 3, including the dimension, grid distribution, and boundary conditions. In Section 4, the mean and turbulence flow over flat terrain and those over a steep 3-D hill will be firstly simulated and the accuracy of these computations will be assessed, then a real complex topography in Japan will be modelled. At last in Section 5 the conclusions of this study will be summarized.

2 NUMERICAL MODEL

2.1 Governing equations

The governing equations are obtained by filtering the time-dependent Navier-Stokes equations in Cartesian coordinates (x, y, z) and expressed in the form of tensor as follows:

$$\frac{\partial \rho \widetilde{u}_i}{\partial x_i} = 0 \tag{1}$$

$$\rho \frac{\partial \widetilde{u}_i}{\partial t} + \rho \frac{\partial \widetilde{u}_i \widetilde{u}_j}{\partial x_j} = \frac{\partial}{\partial x_j}\left(\mu \frac{\partial \widetilde{u}_i}{\partial x_j}\right) - \frac{\partial \widetilde{p}}{\partial x_i} - \frac{\partial \tau_{ij}}{\partial x_j} \tag{2}$$

where $\widetilde{u}_i$ and $\widetilde{p}$ are filtered velocities and pressure respectively, μ is viscosity, ρ is density, τ_{ij} is SGS stress and is modeled as follows:

$$\tau_{ij} = -2\mu_t \widetilde{S}_{ij} + \frac{1}{3}\tau_{kk}\delta_{ij}; \qquad \widetilde{S}_{ij} = \frac{1}{2}\left(\frac{\partial \widetilde{u}_i}{\partial x_j} + \frac{\partial \widetilde{u}_j}{\partial x_i}\right) \tag{3}$$

where, μ_t denotes SGS turbulent viscosity, and $\widetilde{S}_{ij}$ is the rate-of-strain tensor for the resolved scale, δ_{ij} is the Kronecker delta. Smagorinsky-Lilly model is used for the SGS turbulent viscosity:

$$\mu_t = \rho L_s^2 |\widetilde{S}| = \rho L_s \sqrt{2\widetilde{S}_{ij}\widetilde{S}_{ij}}; \qquad L_s = \min(\kappa d, C_s V^{\frac{1}{3}}) \tag{4}$$

in which, L_s denotes the mixing length for subgrid-scales, κ is the von Kármán constant, 0.42, d is the distance to the closest wall and V is the volume of a computational cell. In this study, C_s is Smagorinsky constant and is determined as 0.032 based on Oka and Ishihara (2009).

Finite volume method is used for the present simulations. The second order central difference scheme is used for the convective and viscosity term, and the second order implicit scheme for the unsteady term. SIMPLE (semi-implicit pressure linked equations) algorithm is employed for solving the discretized equations (Ferziger and Peric, 2002).

2.2 Method simulating canopy and roughness block

Liu and Ishihara (2014) has applied a method to simulate the canopy by adding an appropriate momentum source term:

$$f_{\widetilde{u},i} = -\frac{1}{2}\rho C_{D,\widetilde{u}_i} \frac{\gamma_0}{l_0} \widetilde{u}_{mag} \widetilde{u}_i \tag{5}$$

where $C_{D,\widetilde{u}_i}$ is the drag coefficient; γ_0 is the volume occupancy rate; l_0 is the thickness of leaf, and $\widetilde{u}_{mag}$ is the velocity magnitude. $C_{D,\widetilde{u}_i}$, γ_0, and l_0 were chosen as 0.4, 2%, and 1mm, respectively. This value of $C_{D,\widetilde{u}_i}$ is a typical mean value for vegetation canopies as have been mentioned by Kaimal and Finnigan (1994).

For the roughness block which is solid, we can assume it as an extremely dense vegetation canopy. As a result, the same form of source term as eq.(5) could be used again and only the volume occupancy rate, γ_0, is changed to 99.9%.

3 SIMULATION SETUP

3.1 Set up for the flat terrain

In order to evaluate the performance of the numerical wind tunnel, data obtained from an experimental study by Ishihara and Hibi (1998) are used. The experiment was conducted in a return wind tunnel with a test section of 1.1m wide, 0.9m high and 7m long. The neutrally stratified atmospheric boundary layer was simulated using 60mm high cubic elements followed by 20 and 10mm cubic blocks covering 1.2m of the test-section floor. The remaining 5.8 m of the test-section floor was covered with plywood to avoid the complication of the rough to smooth transition. The configuration of the numerical wind tunnel is same as that in experiment except the width of the wind tunnel and the upstream buffer zone, see Fig. 1, where the origin is at the

measured point, 3.4m downstream of the roughness blocks. Mason and Thomson (1987) recommended a spanwise size of approximately 2 times the boundary layer depth as for reproduce the largest eddies. As a result, with consideration of the convenience generating the roughness cubic blocks, 1.8 times of the boundary layer thickness, 0.66m, is determined. The upstream buffer zone, 2.0m long with grid size decreasing from 100mm to 10mm in the flow direction, was appended to avoid any perturbations from the inlet condition into the turbulence generation region. In the test section, two nested domains, i.e., fine grid and coarse grid domain, with a horizontal resolution of 2mm and 10mm, respectively, were used. The fine grid domain starts from 0.5m upstream of the origin and ends at 0.4m downstream with spanwise width 0.2m, and the remaining part of the test section is the coarse grid domain. Same as the experiment, the test section after roughness blocks is covered by using canopy. Considering that the roughness length, z_0, is measured as 0.3mm and the relationship between roughness length and equivalent canopy height is proposed as $k_s=30z_0$ by Ishihara and Hibi (1997), the height of canopy is decided as 9mm. The layers number in the canopy region is 10. From the ground surface to the upper boundary, the grid spacing is same for both fine and coarse grid domains, which was gradually stretched from 0.2mm to 300mm with maximum stretching ratio equaling to 1.2. The total mesh number is 6.8×10^6.

As boundary conditions, a stress-free condition was used at the top of the domain and a symmetry condition at the spanwise sides. Uniform wind flow with a speed of 5.4 m s^{-1} was set at the inlet. At the end of the tunnel outlet boundary condition is applied. No-slip condition for velocity was used at the bottom surface.

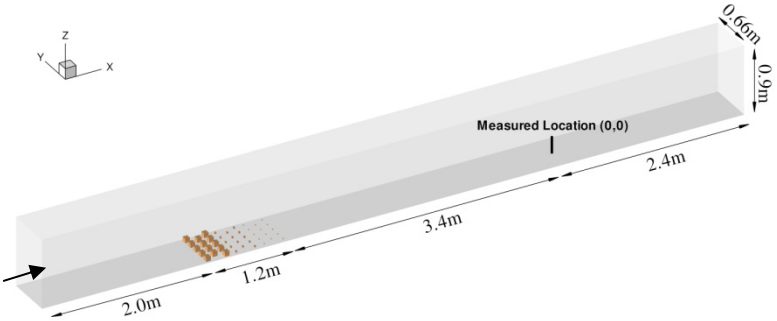

Figure 1: Configuration of numerical model simulating wind tunnel with flat terrain.

3.2 Set up for a 3-D hill

A 3-D hill with a cosine-squared cross section, $z_s(x,y)=h\cos^2(\pi(x^2+y^2)^{1/2}/2L)$, where, h=40mm and L=100mm, is mounted 3.4m downstream of the roughness blocks in the wind tunnel. This wind tunnel is same as the one for the flat terrain case, as shown in Fig.2. A second vertical coordinate $z'=z-z_s$ is also used to describe the height above the local surface. Same grid distribution and boundary conditions as those in the flat terrain case were used. In the vertical direction σ grid method is applied to fit the hill shape. The settings for the boundary conditions are same as those in the first case.

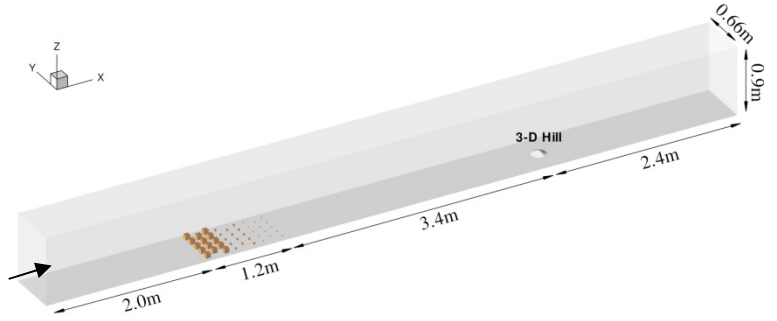

Figure 2: Configuration of numerical model simulating wind tunnel with one 3D hill mounted.

3.3 Set up for a real complex topography

One wind turbine accident occurred in Taikoyama Hill near Kyoto, Japan, as have been reported by Kyoto Prefecture (2013). Some measurement data are available in this wind farm, therefore the very complex topography around Taikoyama Hill, as shown in Fig. 3, is chosen to do examinations. Two 1:2000 topography models with radius R=4km and 8km were made to examine the terrain size effects. The origin of this topography locates at the wind measurement Mast in Taikoyama wind farm. The outer ring of this terrain with width of 1km is used to smooth the surrounding area. A domain with dimensions of 30km×30km×6km (streamwise direction, spanwise direction and vertical direction) was used. The roughness blocks with height of 60m (3cm in scale) were located 12km upstream from the Mast. Fine grid domain is horizontally a square centered at the Mast with side length of 2km. Because the topography in this case is not as hilly as the second case and the simulated area is very wide, a compromise between computational time and accuracy was made, i.e., a relatively coarse resolution of 6m (3mm in scale) is applied in the fine grid domain. Out of the consideration that the averaged height of forest is about 15m as reported by Næsset (1997), this height is used for the canopy height and the number of canopy layers is 10. From the ground surface to the upper boundary, the grid spacing was gradually stretched from 1m to 540m with maximum stretching ratio equaling to 1.2. In the vertical direction σ grid method is applied to fit the hill shape. The total mesh number is 6.2×10^6. The settings for the boundary conditions are same as those in the first case.

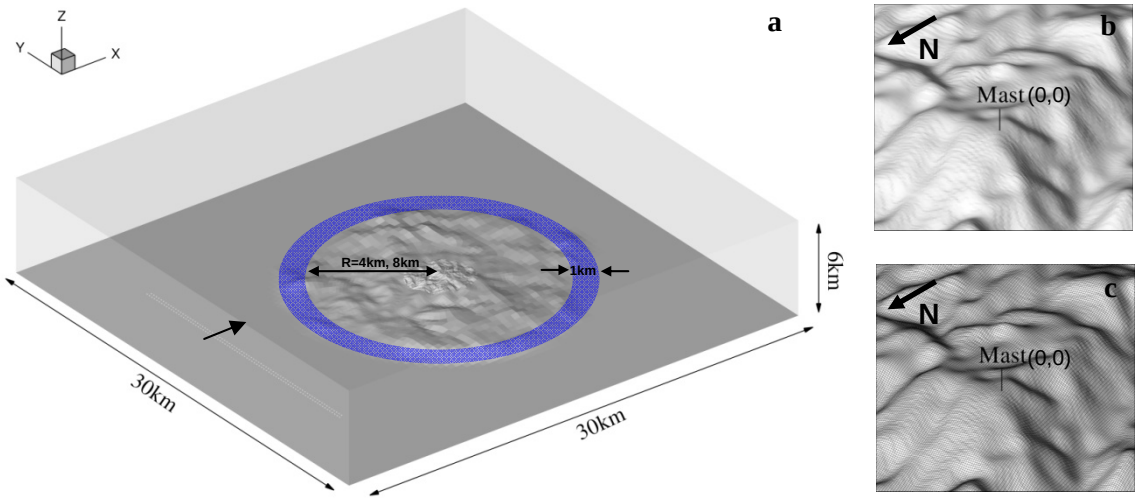

Figure 3: Configuration of numerical model simulating one complex terrain, (a)global view of model; (b) terrain near the Mast; and (c)mesh neat the Mast.

4 NUMERICAL RESULTS AND DISCUSSION

4.1 Flow over the flat terrain

In order to verify the accuracy of the numerical wind tunnel, the method generating turbulence inflow and that simulating canopy, the flow in the undisturbed boundary layer was predicted and compared with the measurements. The vertical profiles of the normalized mean and standard deviation of the streamwise component in the undisturbed boundary layer are shown in Fig. 4, where the referred velocity, U_{ref}, is decided as the wind speed outside the boundary layer, 5.8 m s^{-1}, and the coordinate in vertical direction is normalized by the height of the 3-D hill, h, in the second case. The dashed lines superimposed on Fig.4 indicate the height of canopy. The numerical results show fairly good agreement with the measurements, validating the accuracy of this numerical wind tunnel.

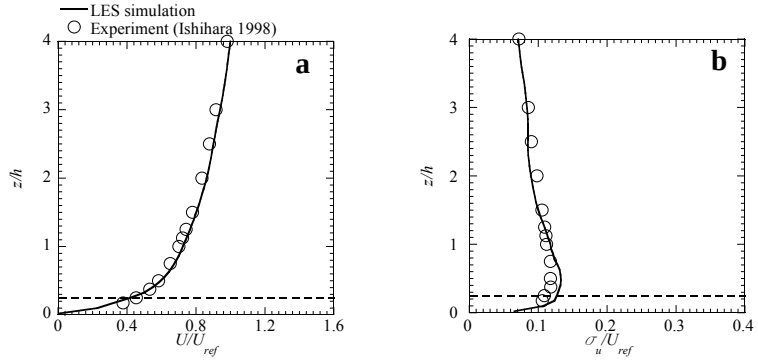

Figure 4: Comparison between predicted and measured, (a) normalized mean streamwise velocity; and (b) normalized streamwise fluctuation; for the flat terrain at x=0h.

4.2 Flow over a 3-D hill

Two representative locations, hill top (x=0h) and far wake (x=5h), are chosen to illustrate the normalized profiles of mean and turbulence streamwise velocity in detail, as shown in Fig. 5 and Fig. 6, respectively. At hill top the speed up of the flow in the simulation is comparable with the experimental data. Because of the drag of canopy, the flow under 0.225h is damped and velocity fluctuation shows peak just at the top of the canopy. The deceleration of the mean wind and the high turbulence at the far wake are well reproduced as could be found in Fig. 6, which implies that the wind characteristics are still influenced by the upstream hill.

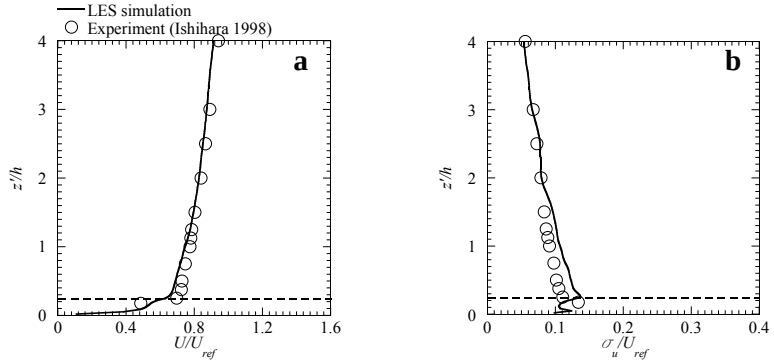

Figure 5: Comparison between predicted and measured, (a) normalized mean streamwise velocity; and (b) normalized streamwise fluctuation; for the 3D-hill at x=0h.

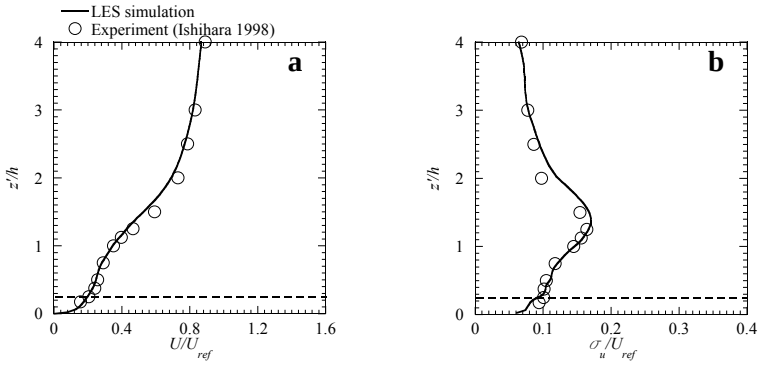

Figure 6: Comparison between predicted and measured, (a) normalized mean streamwise velocity; and (b) normalized streamwise fluctuation; for the 3D-hill at x=5h.

In order to show how strong the influence of the hill is, the whole view of the flow fields is provided in Fig. 7. The distortion of the flow due to the hill especially in the wake region is well captured, but the turbulence in the region of $1.25 \le x/h \le 3.75$ is overestimated. It probably results

from the not enough grid resolution in the wake where the eddies smaller than the grid size may have important mixing effect to reduce the turbulence. The height of shear layer, at which the large gradient of mean streamwise velocity and the peak value of turbulence occur, increases from 1h at x=0h to 1.4h at x=5h. The influence by the hill covers a long distance. This is the indication that in order to well reproduce the flow over a real terrain the tall hills near the measured points should be included in the model.

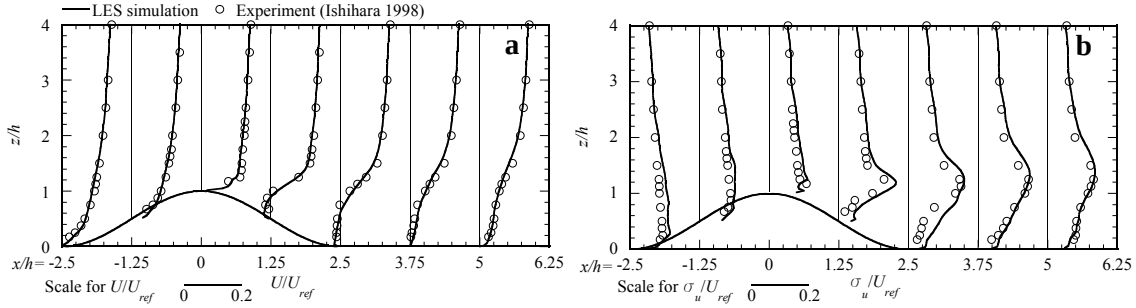

Figure 7: Comparison between predicted and measured, (a) normalized mean streamwise velocity; and (b) normalized streamwise fluctuation; for the 3D-hill from x=-2.5h to x=5h.

4.3 Flow over a real complex terrain

Two models with R=4km and 8km in full scale are simulated under west wind and south wind. Figure 8 shows the comparison between observation and simulation when the wind is from west, in which the reference velocity, U_{ref}, is determined as the mean streamwise velocity at height of 50m. The speedup is captured by both small and large topography models and shows acceptable

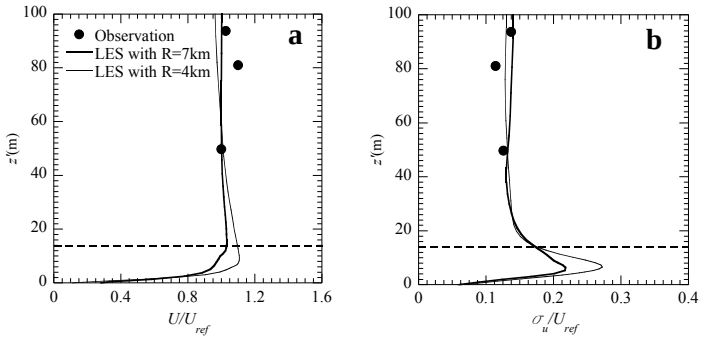

Figure 8: Comparison between observation, simulation with R=4km and simulation with R=8km for the real terrain when the wind is from west, (a) normalized mean streamwise velocity; and (b) normalized streamwise turbulence.

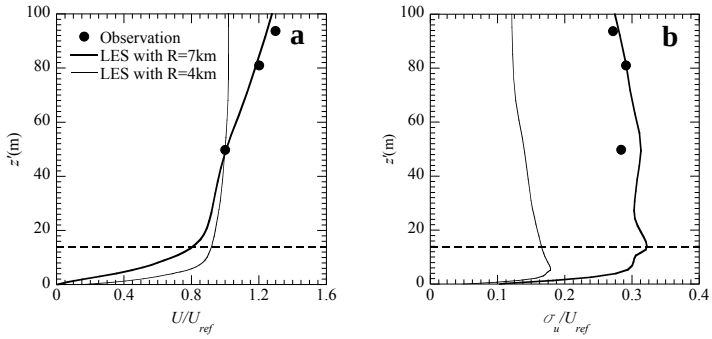

Figure 9: Comparison between observation, simulation with R=4km and simulation with R=8km for the real terrain when the wind is from south, (a) normalized mean streamwise velocity; and (b) normalized streamwise turbulence.

agreement with observed data. This speedup is a typical feature at hill crest as could be seen in Fig. 5(a). Predictions for turbulence wind from these two models are also comparable with observation. However, when the wind is from south, shown in Fig. 9, the small topography model gives very large error, while fairly good agreement is achieved by using large model. The profile of mean streamwise velocity is very similar with that in Fig. 6(a) implying some wake effects from the upstream hill.

In order to explain why both small and large topography models could predict the flow accurately when the wind is from west and why only the large topography can reproduce the observed data when the wind is from south, the sreamwise velocity contours on the vertical crossing section are plotted as shown in Fig. 10 and Fig. 11. If the wind comes from west, the upstream sharp terrain with a maximum slope of 1:1.9, as plotted in Fig. 10(a), gives a mean wind profile similar as that at the hill crest. By comparing between Fig. 10(a) and Fig. 10(b) it could be found even the region exceeding R=4km is cut, where there is no upstream hill taller than the location of the Mast, the flow pattern especially the thickness of the boundary layer is not affected, which is the answer why both small and large topography models could predict the flow accurately when the wind is from west. If the wind comes from south, a hill with almost same altitude, about 550m, could be found 5.5km upstream of the Mast. When the small topography model is used, this tall hill will be smoothed, and from the comparison between Fig. 11(a) and Fig. 11(b), we can clearly identify that the flow pattern are very different. The boundary layer simulated by using large topography is much thicker than that by small topography, indicating that the disturbance due to the upstream tall hill could still influence the flow in the far wake region even with a distance 10 times the height of it. This is the reason why only the large topography can reproduce the observed data when the wind is from south.

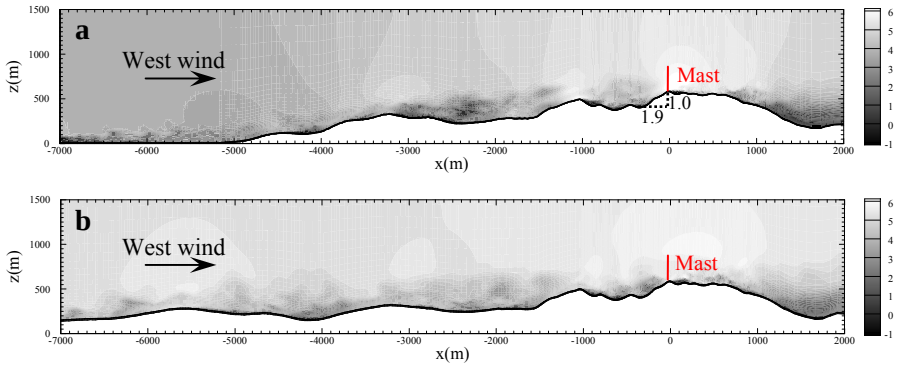

Figure 10: Instantaneous flow fields visualized by streamwise velocity over the terrain with R equals to (a)4km and (b)8km; when the wind is from west.

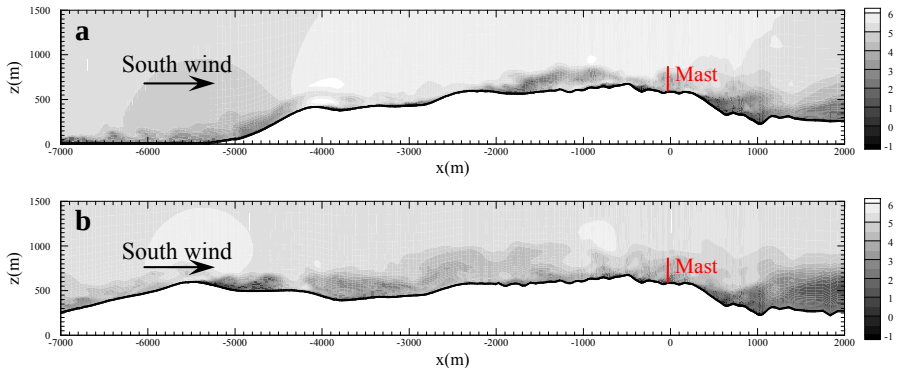

Figure 11: Instantaneous flow fields visualized by streamwise velocity over the terrain with R equals to (a)4km and (b)8km; when the wind is from south.

5 CONCLUSIONS

A numerical investigation on the flow over complex topography has been conducted by using large eddy simulation. The mean and turbulence flow over flat terrain and that over a steep 3-dimensional circular hill in simulation show good agreement with the experimental data, validating the applicability of the proposed numerical wind tunnel. The simulations of a real terrain by two models with difference topography sizes suggest us that even the measured point is located with a distance 10 times the height of an upstream tall hill, the wake effect is still very large and in order to provide a good prediction that tall hill should be included in the simulated region.

References

Cao, S., Wang, T., Ge, Y., Tamura, Y., (2012). Numerical study on turbulent boundary layers over two-dimensional hills—Effects of surface roughness and slope, J. Wind Eng. Ind. Aerodyn., 104-106, p342-349.

Diebold, M., Higgins, C., Fang, J., Bechmann, A., Parlange, M.B., (2013). Flow over hills: A large-eddy simulation of the bolund case, Bound.-Lay. Meteorol., 148, p177-194.

Dupont, S., Brunet, Y., Finnigan, J.J., (2008). Large-eddy simulation of turbulent flow over a forested hill: Validation and coherent structure identification, Q.J.R. Meteorol. Soc., 134, p1911-1929.

Ferreira, A.D., Lopes, A.M.G., Viegas, D.X., Sousa, A.C.M., (1995). Experimental and numerical simulation of flow around two-dimensional hills, J. Wind Eng. Ind. Aerodyn., 54/55, p173-181.

Ferziger, J., Peric, M., (2002). Computational method for fluid dynamics, 3rd Edition, Springer.

Ishihara, T., Hibi, K., (1997). Turbulent characteristics of flow field over a three-dimensional steep hill, J. of Wind Eng., 73, p3-14. (In Japanese)

Ishihara, T., Hibi, K., (1998). An experimental study of turbulent boundary layer over steep hills, Proc. of 15th National Sym. on Wind Eng., p61-66. (In Japanese)

Ishihara, T., Hibi, K., (2002). Numerical study of turbulent wake flow behind a three-dimensional steep hill, Wind Struct., 5, p317-328.

Kaimal, J.C., Finnigan, J.J., (1994). Atmospheric boundary layer flows - their structure and measurements, Oxford University Press, New York.

Kobayashi, M.H., Pereira, J.C.F., Siqueira, M.B.B., (1994). Numerical study of the turbulent flow over and in a model forest on a 2D hill, J. Wind Eng. Ind. Aerodyn., 53, p357-374.

Kyoto Prefecture, (2013). 京都府太鼓山風力発電所３号機ナセル落下事故報告. (In Japanese)

Liu, Z., Ishihara, T., (2014). LES modeling of canopy flows for wind prediction in urban area (submitted to Proc. of RE2014)

Lopes, A.S., Palma, J.M.L.M., Castro, F.A., (2007). Simulation of the Askervein flow. Part 2: Large-eddy simulations, Bound.-Lay. Meteorol., 125, p85-108.

Mason, P.J., Thomson, D.J., (1987). Large-eddy simulations of the neutral-static-stability planetary boundary layer, Q.J.R. Meteorol. Soc., 113, p413-443.

Næsset, E., (1997). Determination of mean tree height of forest stands using airborne laser scanner data, J. Photogrammetry Remote Sens., 52, p49-56.

Oka, S., Ishihara, T., (2009). Numerical study of aerodynamic characteristics of a square prism in a uniform flow. J. Wind Eng. Ind. Aerodyn., 97, p548-559.

Tamura, T., Okuno, A., Sugio, Y., (2007). LES analysis of turbulent boundary layer over 3D steep hill covered with vegetation, J. Wind Eng. Ind. Aerodyn., 95, p1463-1475.